

Highlighting joint research results from Jinhui Liu's Group, the Research Center for Biomimetic Functional Materials and Sensing Devices, Institute of Intelligent Machines, Chinese Academy of Sciences, Hefei, Anhui, China.

Title: Novel hybridized SWCNT-PCD: synthesis and host-guest inclusion for electrical sensing recognition of persistent organic pollutants

The fabricated electrical sensor based on SWCNT-PCD hybrids has been successfully used for electrical recognition of POPs, displaying excellent sensitivity and selectivity due to the concept of molecular recognition. It is reasonable to believe that the hybridized SWCNT-PCD sensor holds great potential to be developed as a real time environmental monitor.

As featured in:



See L. Kong *et al.*,
J. Mater. Chem., 2011, **21**, 11109.

RSC Publishing

www.rsc.org/materials

Registered Charity Number 207890

Cite this: *J. Mater. Chem.*, 2011, **21**, 11109

www.rsc.org/materials

PAPER

Novel hybridized SWCNT–PCD: synthesis and host–guest inclusion for electrical sensing recognition of persistent organic pollutants†

Lingtao Kong, Jin Wang,* Fanli Meng, Xing Chen, Zhen Jin, Mingqiang Li, Jinhui Liu* and Xing-Jiu Huang*

Received 28th December 2010, Accepted 27th April 2011

DOI: 10.1039/c0jm04552g

Fabrication of a hybridized single-walled carbon nanotube (SWCNT) device based on novel sensing material mono-6-deoxy-6-(*p*-aminophenylamino)- β -cyclodextrin (PCD) *via* a facile approach has been reported for the first time; moreover, the hybridized material PCD-decorated SWCNTs (SWCNT–PCD) can be characterized by ultraviolet–visible–near infrared spectroscopy, Raman spectroscopy, thermogravimetric analysis, field-emission scanning electron microscopy and high resolution transmission electron microscopy. The PCD-decorated SWCNT devices have been employed to detect Persistent Organic Pollutants (POPs) on the basis of formation of an inclusion complex with guest molecules between SWCNT–PCD and POPs, such as 2,4,5-trichlorobiphenyl (TCB), *etc.* The significant variation of the electrical conductance of the SWCNT–PCD hybrid corresponding to the presence of several POPs with different adsorption efficiencies on the surface indicates that the hybrid is highly sensitive to some specific POP molecules, implying that hybridized SWCNT–PCD has great potential in application as an environmental monitor. In order to make a quantitative assessment of the inclusion complexation behavior of PCD with these POP molecules, microcalorimetric titration experiments and discussions have been carried out.

1. Introduction

According to the “Stockholm convention on POPs (persistent organic pollutants)” founded on the United Nations Conference in 2001, the usage of POPs has been strictly restricted. Therefore, it is very important to detect and treat POPs, *e.g.*, 2,4,5-trichlorobiphenyl (TCB), hexachlorobenzene (HCB), aldrin, mirex and chlordane (CD-68), in that these highly noxious chemicals have been widely-spread in the environment and accumulated in organisms. Although many detection approaches have been developed, *e.g.*, chromatography,¹ electrochemical methods,² and surface-enhanced Raman scattering (SERS),³ exploring and developing facile and rapid approaches combined with novel hybridized nanomaterials for the sensitive detection of POPs is currently a major challenge. Most recently, the facile electrical detection of several target POPs through porous SnO₂ nanostructures has been developed first by our group;⁴ however, the sensitivity and selectivity need to be improved.

As is well known, single-walled carbon nanotubes (SWCNTs) have been considered as chemical nanosensor materials for detecting analytes^{5–12} due to their unique quasi-

one-dimensional electronic structures and very high surface-to-volume ratios.^{13–20} Unfortunately, the poor sensitivities and selectivities of undecorated SWCNTs severely limit their application in detection of POPs. Therefore, in order to improve the sensing performance of SWCNTs,^{21,22} the functionalization of SWCNTs *via* physical or chemical approaches is currently attracting much attention because chemical functionalization can enhance both processibility and sensing performance of the SWCNTs; moreover, it can improve dissolution and dispersion of the SWCNTs in various solvents,^{23,24} which opens the door to cost-effective methods for the fabrication of sensors using simple dispensing or printing techniques.

Hence, a new strategy, *i.e.*, SWCNTs decorated with mono-6-deoxy-6-(*p*-aminophenylamino)- β -cyclodextrin (PCD) (Fig. 1), has been applied to obtain novel hybridized chemosensors for detection of POPs thanks to its special molecular structure, that is, a hydrophobic internal cavity and a hydrophilic external surface for molecular recognition.^{25–30} This route can greatly improve sensitivity and selectivity for detecting organic molecules.^{31–36} It can be expected that an inclusion complex with guest molecules can be efficiently formed between PCD decorated SWCNTs and POPs, such as TCB, CD-68, aldrin and HCB *etc.* Therefore, synthesis of PCD and fabrication of PCD-decorated SWCNTs (SWCNT–PCD) hybrid devices, which behave as electrical sensors that are chemically specific and capable of detecting nanomolar concentrations of TCB, are reported in the present paper.

Research Center for Biomimetic Functional Materials and Sensing Devices
Institute of Intelligent Machines, Chinese Academy of Sciences, Hefei,
Anhui, 230031, China. E-mail: jwang@iim.ac.cn; jhliu@iim.ac.cn;
xingjiuhuang@iim.ac.cn; Fax: +86-551-5592420

† Electronic supplementary information (ESI) available. See DOI:
10.1039/c0jm04552g

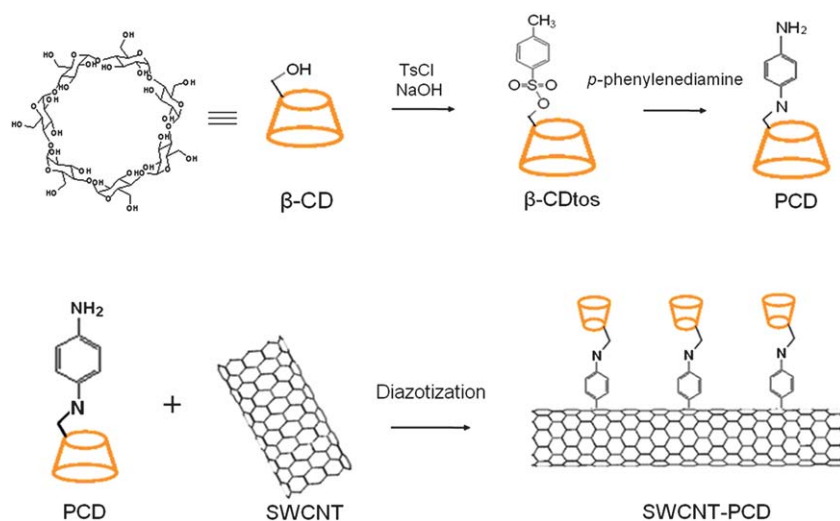


Fig. 1 Schematic representation of synthesis of PCD and preparation of SWCNT-PCD hybrids.

2. Experimental

2.1 Materials and chemicals

β -cyclodextrin (β -CD) (95%) was purchased from Sinopharm Chemical Reagent Co., Ltd., China. *p*-Phenylenediamine (98%), *p*-toluenesulfonyl chloride (TsCl) (95%) and all other chemicals (analytical pure grade) were obtained from Shanghai Chemical Co. Ltd. China. The SWCNTs (CVD) used in this study were purchased from Shenzhen Nanotech Port Co. Ltd. China. The purity was declared to be above 95%.

2.2 Instruments

Fourier transform infrared (FT-IR) spectra were recorded on a Nexus-870 spectrophotometer. Nuclear magnetic resonance (NMR) spectra were acquired at 25 °C using a Bruker Avance spectrometer. Elemental analysis for C, H, and N was performed using an Elementar Vario EL-III analyzer. Ultraviolet visible near infrared (UV-Vis-NIR) absorption spectra were recorded by using a Solidspec-3700 spectrophotometer. Field-emission scanning electron microscopy (FESEM) images were taken by a Sirion 200 field-emission scanning electron microscope. High resolution transmission electron microscopy (HRTEM) images were obtained from a JEOL JEM-2010 instrument operated at 100 kV. Thermogravimetric analysis (TGA) was performed using a Shimadzu TGA-50H analyzer in argon surroundings. Raman spectra were collected from a DXR Smart Raman Spectrometer using 25 mW of 514 nm radiation from a helium neon laser. Integration times were provided as 30 s.

2.3 Preparation of mono-6-deoxy-6-(*p*-tolylsulfonyl)- β -Cyclodextrin (β -CDtos)

β -CD (70 g) was suspended in water (500 mL), and 20 mL aqueous solution including NaOH (6.6 g) was added dropwise to the β -CD suspension so that the suspension gradually became transparent. *p*-Toluenesulfonyl chloride (10 g) in acetonitrile (30 mL) was added dropwise to the transparent solution so as to form a white precipitate. After stirring for 2 h at ambient

temperature, the precipitate could be removed by suction filtration and the filtrate was refrigerated for a couple of days at 4 °C. The white precipitate was recovered *via* suction filtration and recrystallized twice to obtain a pure white solid. ^1H NMR (400 MHz, $(\text{CD}_3)_2\text{SO}$, 25 °C, TMS, δ): 2.43 (s, 3 H), 3.20–3.40 (m, overlaps with HOD), 3.44–3.66 (m, 28 H), 4.17–4.52 (m, 6 H), 4.77 (s, 3 H), 4.84 (s, 4 H), 5.64–5.84 (m, 14 H), 7.43 (d, $J = 8.07$ Hz, 2 H), 7.75 (d, $J = 8.11$ Hz, 2 H) ppm. Anal. calcd (%) for $\text{C}_{49}\text{H}_{76}\text{O}_{37}\text{S} \cdot 3\text{H}_2\text{O}$: C, 43.81; H, 6.15; S, 2.39. Found (%): C, 43.58; H, 6.21; S, 2.28.

2.4 Preparation of mono-6-(*p*-aminophenylamino)- β -cyclodextrin (PCD)

β -CDtos (4.0 g) and *p*-phenylenediamine (0.8 g) were dissolved in water (30 mL) containing triethylamine (20 mL), and the stirred mixture was heated to reflux under a nitrogen atmosphere for 24 h. After evaporation under reduced pressure, the residue was poured into vigorously stirred anhydrous ethanol (500 mL), and the resultant mixture was stored in a refrigerator to produce a slight red precipitate. The crude solid product was collected by filtration and then purified by column chromatography on a hydroxymethylcellulose column with an aqueous ammonium bicarbonate eluent (0.05 M), followed by chromatography on a Sephadex G-25 column with deionized water as the eluent, to give the product (2.2 g) in 50% yield. ^1H NMR (400 MHz, $(\text{CD}_3)_2\text{SO}$, 25 °C, TMS, δ): 3.20–3.45 (m, overlaps with HOD), 3.52–3.66 (m, 28 H), 4.20–4.63 (m, 6 H), 4.83–4.88 (s, 7 H), 5.57–5.95 (m, 14 H), 6.39 (d, $J = 8.48$ Hz, 2 H), 6.43 (d, $J = 8.42$ Hz, 2 H) ppm. Anal. calcd (%) for $\text{C}_{48}\text{H}_{76}\text{N}_2\text{O}_{34} \cdot 7\text{H}_2\text{O}$: C, 42.67; H, 6.71; N, 2.07. Found (%): C, 42.36; H, 6.59; N, 2.23.

2.5 Purification and disentanglement of SWCNTs

100 mg SWCNT raw soot was first heated in air at 350 °C for 3 h. The remaining soot was sonicated in 30 mL 37 wt% hydrochloric acid for 4 h and then refluxed for 5 h. The solution was filtered using a 0.20 μm Teflon filter under vacuum. The sediment was washed with copious water, and then it was vacuum-dried at

60 °C for one day. Disentanglement of the SWCNT bundles was performed by oleum. The obtained SWCNTs were soaked in oleum (20% SO₃) for 72 h using an immersion blender so that the intercalation of acid into the tightly entangled network of SWCNTs would loosen the ropes. After diluting with deionized water, the mixture was centrifuged and the supernatant acid was decanted off. The precipitate was washed with deionized water three times and then ultrasonically dispersed into 20 mL 0.2% benzalkonium chloride solution. The solution was centrifuged at 4000 rpm for 20 mins. The supernatant solution was filtrated with a 0.20 μm Teflon filter under vacuum, washed extensively with deionized water until the pH of the filtrate reached 6 and dried under vacuum. Finally, the purified SWCNTs were obtained by annealing in Ar at 900 °C for 30 min to remove the oxygen-based functional groups generated from the oleum treatment. Approximate 25 mg of product was obtained.

2.6 Preparation of SWCNT–PCD hybrids

In a typical experiment, 6 mg of the purified SWCNTs was sonicated for 30 min in 10 mL of DMF. A solution of 100 mg PCD (0.4 mmol) in 3 mL of DMF was added to the suspension. After transferring to a septum-capped reaction flask and bubbling with nitrogen for 10 min, 0.1 mL of isoamyl nitrite was quickly added. The suspension was stirred in the dark at 70 °C for 24 h. After being cooled to room temperature, the suspension was diluted with 30 mL DMF, filtered through a 0.2 μm Teflon filter, and washed extensively with DMF until the filtrate became colorless. Subsequently, it was dried in vacuum at 80 °C for 24 h to give a black powder of the modified SWCNTs (5 mg).

2.7 Preparation of electrode

The electrodes for the sensors were microfabricated on a silicon substrate using standard lithographic patterning. A one micron thick SiO₂ film was initially deposited on a (100) oriented silicon wafer to insulate the substrate using chemical vapor deposition (CVD). After photo lithographically defining the electrode area, a Cr adhesion layer and a *ca.* 300 nm-thick Au layer were evaporated *via* e-beam. Finally, the electrodes were defined using lift-off techniques.

The obtained electrodes were cleaned for 45 min in hot Piranha solution H₂O₂–H₂SO₄ (3 : 1, v/v), rinsed copiously with water, and dried under N₂. Self-assembled monolayers of aminopropyltriethoxy silane (APTES) were absorbed from 1% solution in anhydrous toluene (AHT) for one hour at room temperature, followed by rinsing and sonication with AHT and drying under N₂.

2.8 Microcalorimetric titration

The microcalorimetric titrations were performed at atmospheric pressure and 25 °C in H₂O–MeOH (9 : 1, v/v) solution by using Microcal VP-ITC titration microcalorimetry. All solutions were degassed and thermostated using a thermostat accessory before the titration experiment. In each run, a H₂O–MeOH solution of PCD host (2.00 mM) in a 0.30 mL syringe was sequentially injected with stirring at 500 rpm into the calorimeter sample cell containing a H₂O–MeOH solution of POP guests. The sample cell volume was 1.430 mL in all experiments. Each titration

experiment was composed of 34 successive injections (8 μL per injection). POP solutions were applied at a concentration between 0.05 and 0.1 mM. In the microcalorimetric titration experiments, each titration of PCD into the sample cell gave rise to a heat of reaction, caused by the formation of inclusion complexes between POP molecules and PCD. The heats of reaction decrease after each injection of PCD because the quantity of POP molecules available for forming inclusion complexes is decreased. The dilution heat of titrant and analytes has been measured and deducted in all ITC experiments.

3. Results and discussion

3.1 Characterization of SWCNT–PCD hybrids

PCD has been synthesized through a two-step reaction (Fig. 1), *i.e.*, preparation of mono-6-deoxy-6-(*p*-toylsulfonyl)-β-cyclodextrin (β-CDtos) from β-cyclodextrin and *p*-toluenesulfonyl chloride in aqueous solution including NaOH as the first step, PCD was subsequently synthesized by the condensation of β-CDtos with *p*-phenylenediamine in water in the presence of triethylamine as a catalyst. The SWCNTs were functionalized with PCD *via* the *in situ* generation of the corresponding aryl diazonium of PCD. The CD (cyclodextrin) group is covalently attached to the surface of the SWCNTs with the aid of a benzene ring between the two moieties (Fig. 1). The structure, properties and morphologies of the SWCNT–PCD hybrids can be comprehensively analyzed by Raman spectroscopy, thermogravimetric analysis (TGA), ultraviolet–visible–near infrared (UV-Vis-NIR), field-emission scanning electron microscopy (FESEM) and high resolution transmission electron microscopy (HRTEM).

The Raman spectra of the bare SWCNTs and SWCNT–PCD hybrids are shown in Fig. 2A. The degree of functionalization can be preliminarily reflected in intensity of the D-band.³⁷ After functionalization with PCD, the relative intensities of three main modes are changed. Compared to the tangential mode (G-band) at *ca.* 1590 cm⁻¹, the intensity of the radial breathing mode (RBM) (*ca.* 160, 210, and 270 cm⁻¹) is slightly decreased; however, the intensity of the disorder mode (D-band) at *ca.* 1290 cm⁻¹ is significantly increased, and the D/G ratio value increases from 0.08 (bare SWCNTs) to 0.2 (SWCNT–PCD). The increase in the relative intensity of the D-band can be attributed to an increased number of sp³-hybridized carbons in the nanotube framework.³⁷

The removal of functional moieties from the pristine SWCNTs in the inert environment by sufficient heating leads to mass loss in the TGA measurements, which can be used to quantitatively estimate the functionalization degree of the carbon nanotubes. When SWCNT–PCD hybrids are heated to 750 °C in an argon atmosphere (10 °C min⁻¹), the total mass loss in the TGA experiment is *ca.* 36% (about 29% between 300–400 °C); moreover, PCD has been efficiently functionalized on the SWCNTs which is reflected in the higher decomposition temperature of the SWCNT–PCD hybrids compared to that of PCD (Fig. 3). Again, the Raman spectrum of SWCNT–PCD after the TGA experiment (Fig. 2B) is found to be quite similar to that of pristine SWCNTs, indicating that only intact nanotubes are left if the functional moieties are removed.

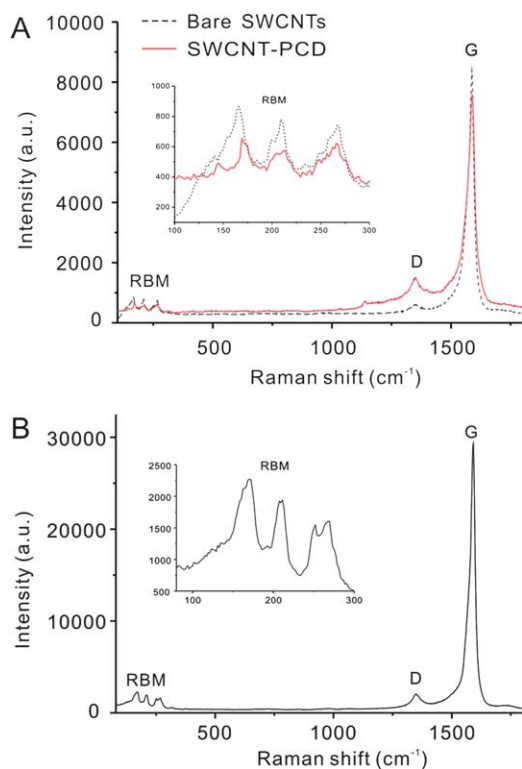


Fig. 2 Raman spectra (514 nm excitation) of SWCNTs, A) bare SWCNTs and SWCNT-PCD. B) SWCNT-PCD after 750 °C TGA treatment in an argon atmosphere at 10 °C min⁻¹. The insets show the magnified RBM bands.

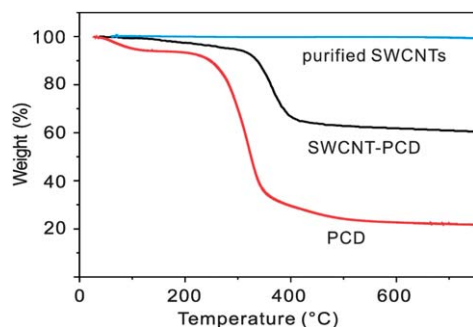


Fig. 3 TGA of the purified SWCNTs, PCD and SWCNT-PCD hybrids in an argon atmosphere (10 °C min⁻¹; incipient sample mass: 1.283, 2.277 and 1.402 mg for the purified SWCNTs, PCD and SWCNT-PCD hybrids, respectively; crucible type: alumina, 150 μ L).

In addition to Raman and TGA, the functional degree of the SWCNTs can also be evaluated by UV-Vis-NIR absorption experiments. A high degree of covalent functionalization gives rise to the disappearance of van Hove singularities of the SWCNTs, which can be attributed to the disruption of the delocalized π -conjugation in the sp^2 -hybridized nanotubes.³⁸ However, the specific van Hove singularities in the present SWCNT-PCD hybrids are partially retained (Fig. 4), indicating that the π -conjugated electron structures of the SWCNTs are not severely damaged.^{39,40} In addition, the disappearance of the band at *ca.* 550 nm in the UV-Vis-NIR absorption spectrum of

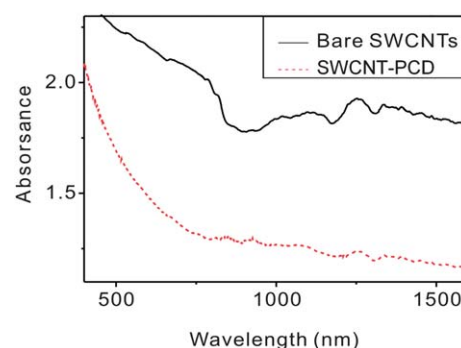


Fig. 4 UV-Vis-NIR absorption spectra of bare SWCNTs and SWCNT-PCD in DMF.

SWCNT-PCD suggests that metallic SWCNTs in the sample are basically destroyed,⁴¹ which implies that metallic SWCNTs are preferentially diazotized.⁴²

The bare and functionalized SWCNTs can be directly observed using FESEM. As shown in Fig. 5A, most of the SWCNTs are easily entangled so as to form large-sized nanotube bundles. In contrast, PCD decorated SWCNTs can be effectively exfoliated (Fig. 5B) and well dispersed in dimethylformamide (DMF), which may be related to the larger solubility of SWCNT-PCD in DMF compared to bare SWCNTs. Moreover, no precipitation or flocculation in the saturated solution of the SWCNT-PCD hybrids can be observed over several months. Besides, the HRTEM image of SWCNT-PCD (Fig. 5C) shows the presence of individual SWCNTs with rugged surfaces, which has been ascribed to the attachment of cyclodextrin functional groups to the tube wall.

3.2 Protocol and sensing behavior of SWCNT-PCD hybridized devices

As shown in schematic graph (Fig. 6), an SWCNT-PCD film was spin-coated from 10 μ g mL⁻¹ DMF solution onto a silicon substrate with one micron thick SiO₂ dielectric and interdigital gold electrodes (300 nm thickness, 5 μ m gap distance), which had been previously self-assembled with a monolayer of amino-propyltriethoxy silane (APTES). Aminosilanes are used because they can enhance the absorption and localization of nanotubes.⁴³ The resistance of SWCNT-PCD devices range from 1 to 1.2 M Ω . It is very important to control the quality of the dispersions so as to ensure that the SWCNT-PCD hybrids form percolative networks of largely individual tubes.

A cyclodextrin derivative was chosen to be attached to SWCNTs due to its hydrophobic inner cavity and hydrophilic outer surface, which acts as a good receptor for organic substrates in aqueous solution. Herein, SWCNT-PCD hybrids have been prepared and fabricated as sensing devices for the detection of POPs (TCB, aldrin, mirex, HCB, and CD-68). These molecules can be included inside the cavities of CD with different binding affinities. The SWCNT-PCD sensing device was soaked in H₂O-MeOH (9 : 1, v/v) solutions of POPs for 1 h, and the POPs molecules enter the cavities of CD (Fig. 6), they were afterwards washed with H₂O, and finally dried in a vacuum oven (60 °C) for 30 min to remove residual solvent.

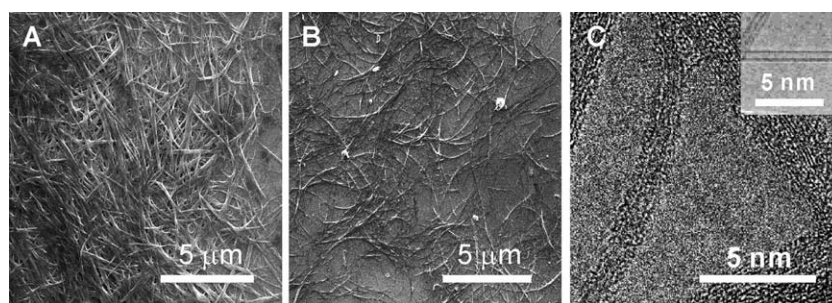


Fig. 5 (A) FESEM image of bare SWCNTs showing the bundles of nanotubes. (B) FESEM image of SWCNT-PCD showing exfoliation of nanotubes. (C) HRTEM image of SWCNT-PCD. The inset is a TEM image of individual pristine SWCNTs.

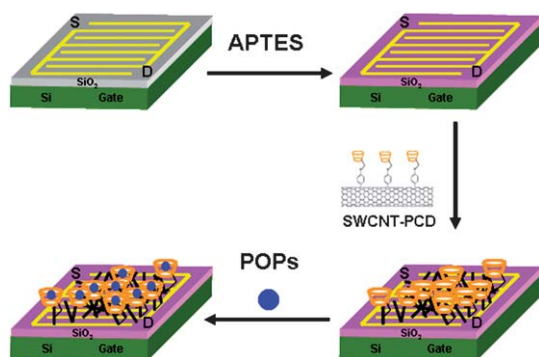


Fig. 6 Schematic view of sensor structure and its interaction with POPs.

Attention now turns to the study of the electrical behavior of SWCNT-PCD sensing devices for POPs. The current-voltage (I - V) curves were measured *via* a picoammeter voltage source-meter (Keithley 6487, USA) with a bias voltage from -2 to $+2$ V between the two electrodes at room temperature. The typical I - V curves of hybrid SWCNT-PCD devices before and after binding TCB and CD-68 are displayed in Fig. 7. It has been found that after binding with the POP molecules the conductance of the SWCNT-PCD hybrid networks decreases; however, in the control tests, only H_2O -MeOH solution without POPs and bare SWCNTs were used instead of SWCNT-PCD (data not shown), and the conductance hardly changed. This suggests that the POP molecules captured in the cavities will cause a rearrangement in the charge distribution of the CD moieties in the SWCNT-PCD hybrids, and induce charge transfer from the CD molecules to the SWCNTs, which leads to the decrease in charge carrier density in the p-type semiconducting SWCNTs. On the other hand, the POP molecules captured in the CD cavities can engender a further decrease of the charge mobility in SWCNTs either by altering the scattering potentials of the CD molecules or by causing further deformation of the SWCNTs.^{44,45} In addition, by binding different POPs at the same concentration, 500 nM, different conductance change ratios (CCRs) of the SWCNT-PCD hybrid networks can be obtained; *ca.* 1.6% for HCB, *ca.* 3.3% for mirex, *ca.* 3.8% for CD-68, *ca.* 5.6% for aldrin, and *ca.* 12.5% for TCB.

Further, the detection of TCB was performed at different concentrations. As shown in Fig. 8, the CCR of SWCNT-PCD hybrid networks obtained is *ca.* 1.7% even at 25 nM, suggesting that the sensing can be qualified as having a nanomolar level of sensitivity.

3.3 Sensing mechanism of SWCNT-PCD hybrids for detecting POPs

The number of captured POP molecules directly depends on their binding abilities towards the CD cavities. In order to make a quantitative assessment of the inclusion complexation behavior of the PCD with these POP molecules, microcalorimetric titration experiments were performed using Microcal VP-ITC titration microcalorimetry, which allowed us to determine simultaneously the standard enthalpy changes (ΔH°), entropy changes (ΔS°) and equilibrium constant (K) (Table S1 in the ESI[†]). Typical titration curves of host PCD with guest TCB are shown in Fig. 9.

The values of K , Gibbs free energy change (ΔG°) ($\Delta G^\circ = -RT \ln K = \Delta H^\circ - T \Delta S^\circ$, where R is the gas constant,

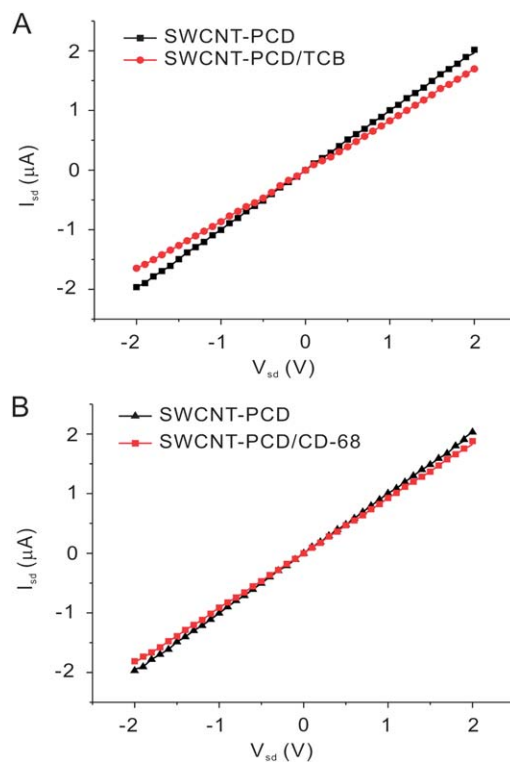


Fig. 7 The current-voltage (I - V) curves of the SWCNT-PCD sensing devices before and after binding of the POP molecules at concentrations of 500 nM (A for TCB, B for CD-68).

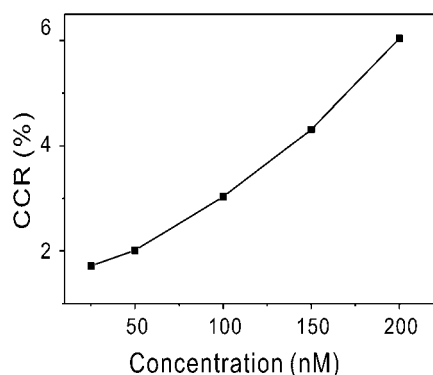


Fig. 8 CCR (conductance change ratio) of the SWCNT–PCD sensing devices in response to TCB in different concentration solution.

$T = 298.15$ K) obtained for the complexation of PCD with POPs, and the CCR of the SWCNT–PCD devices before and after binding of these POPs are listed in Table 1. The K values for the complexation of PCD with these POPs exhibit the following sequence of binding abilities: TCB > aldrin > CD-68 > mirex > HCB; moreover, the K values correlate with the magnitudes of the CCRs of the SWCNT–PCD devices before and after binding of these POP molecules. After plotting the complex formation constants *versus* the values of the CCR of the SWCNT–PCD devices, a good linear relationship with a correlation coefficient of 0.997 can be found. The variance of change in the CCR of the SWCNT–PCD devices depends on the quantities of guest

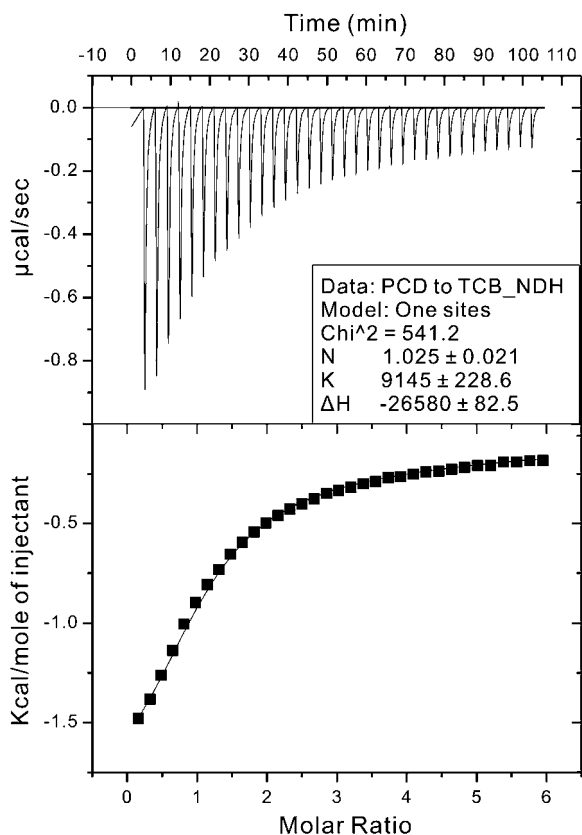


Fig. 9 Calorimetric titration curves of host PCD with guest TCB.

Table 1 Values of the CCR (conductance change ratio) of SWCNT–PCD devices before and after binding of POPs, to reflect their sensing towards different POP molecules the K and $-\Delta G^\circ$ when PCD forms complexes with these POP molecules can be compared

POPs	CCR/%	K/M^{-1}	$-\Delta G^\circ/kJ\ mol^{-1}$
TCB	12.5	9145 ± 229	22.59 ± 0.07
Aldrin	5.6	3613 ± 42	20.3 ± 0.03
CD-68	3.8	2667 ± 82	19.55 ± 0.08
Mirex	3.3	1968 ± 15	18.8 ± 0.03
HCB	1.6	823 ± 36	16.63 ± 0.1

molecules included in the host cavities, suggesting that the SWCNT–PCD hybrid devices can be used for selective sensing recognition of POPs.

4. Conclusions

In summary, novel SWCNT–PCD hybrids have been successfully synthesized through an *in situ* diazonium reaction between SWCNTs and PCD. The results reveal that the one-dimensional electronic structures of the functionalized tubes could basically be maintained without damaging their electronic properties. In comparison with our recent results, the fabricated electrical sensor based on SWCNT–PCD hybrids has been successfully used to detect POPs, and it displays excellent sensitivity and selectivity due to the concept of molecular recognition. The K values for the complexation of the PCD with the different POPs correlate with the magnitudes of the CCRs of the SWCNT–PCD device after binding with these POP molecules. Another important advantage is that the present sensing device overcomes the limitation of some chemical signal-based methods caused by the inactivity of POPs. It is reasonable to believe that the hybridized SWCNT–PCD sensor holds great potential to be developed as a real time environmental monitor.

Acknowledgements

This work is supported by the One Hundred Person Project of the Chinese Academy of Sciences (CAS), China, the National Basic Research Program of China (Grant No. 2007CB936603), The National Key Scientific Program–Nanoscience and Nanotechnology (Grant No. 2011CB933700), and the National Natural Science Foundation of China (Grant Nos. 20875004, 21075002 and 61071054). Dr Jin Wang thanks the National Natural Science Foundation of China (Grant No. 21077106) and Innovation Project of Chinese Academy of Sciences (KCX2-YW-G-058) for financial support.

References

- 1 S. P. J. van-Leeuwen and J. de Boer, *J. Chromatogr., A*, 2008, **1186**, 161.
- 2 S. Rubio and D. Perez-Bendito, *Anal. Chem.*, 2009, **81**, 4601.
- 3 Y. Yang and G. Meng, *J. Appl. Phys.*, 2010, **107**, 044315.
- 4 J. Y. Liu, F. L. Meng, T. Luo, W. Li, M. Q. Li and J. H. Liu, *Talanta*, 2010, **82**, 409.
- 5 P. F. Qi, O. Vermesh, M. Grecu, A. Javey, Q. Wang and H. J. Dai, *Nano Lett.*, 2003, **3**, 347.
- 6 K. H. An, S. Y. Jeong, H. R. Hwang and Y. H. Lee, *Adv. Mater.*, 2004, **16**, 1005.

- 7 A. Star, T.-R. Han, V. Joshi, J.-C. P. Gabriel and G. Grüner, *Adv. Mater.*, 2004, **16**, 2049.
- 8 C. Y. Lee, R. Sharma, A. D. Radadia, R. I. Masel and M. S. Strano, *Angew. Chem., Int. Ed.*, 2008, **47**, 5018.
- 9 X. Peng and S. S. Wong, *Adv. Mater.*, 2009, **21**, 625.
- 10 L. T. Kong, J. Wang, T. Luo, F. L. Meng, X. Chen, M. Q. Li and J. H. Liu, *Analyst*, 2010, **135**, 368.
- 11 E. S. Forzani, X. L. Li, P. M. Zhang, N. J. Tao, R. Zhang, I. Amlani, R. Tsui and L. A. Nagahara, *Small*, 2006, **2**, 1283.
- 12 L. T. Kong, J. Wang, X. C. Fu, Y. Zhong, F. L. Meng, T. Luo and J. H. Liu, *Carbon*, 2010, **48**, 1262.
- 13 J. Kong, M. G. Chapline and H. J. Dai, *Adv. Mater.*, 2001, **13**, 1384.
- 14 J. Yan, Y. C. Zhou, P. Yu, L. Su, L. Q. Mao, D. Q. Zhang and D. B. Zhu, *Chem. Commun.*, 2008, 4330.
- 15 S. Erbas, A. Gorgulu, M. Kocakusakogullaric and E. U. Akkaya, *Chem. Commun.*, 2009, 4956.
- 16 B. L. Allen, P. D. Kichambare and A. Star, *Adv. Mater.*, 2007, **19**, 1439.
- 17 T. Zhang, S. Mubeen, N. V. Myung and M. A. Deshusses, *Nanotechnology*, 2008, **19**, 332001.
- 18 D. L. Fu, H. Lim, Y. M. Shi, X. C. Dong, S. G. Mhaisalkar, Y. Chen, S. Moochhala and L. J. Li, *J. Phys. Chem. C*, 2008, **112**, 650.
- 19 E. S. Snow, F. K. Perkins, E. J. Houser, S. C. Badescu and T. L. Reinecke, *Science*, 2005, **307**, 1942.
- 20 Q. Cao and J. A. Rogers, *Adv. Mater.*, 2009, **21**, 29.
- 21 E. Bekyarova, M. Davis, T. Burch, M. E. Itkis, B. Zhao, S. Sunshine and R. C. Haddon, *J. Phys. Chem. B*, 2004, **108**, 19717.
- 22 M. Castro, J. Lu, S. Bruzaud, B. Kumar and J. F. Feller, *Carbon*, 2009, **47**, 1930.
- 23 A. A. Stefopoulos, C. L. Chochos, M. Prato, G. Pistolis, K. Papagelis, F. Petraki, S. Kennou and J. K. Kallitsis, *Chem.–Eur. J.*, 2008, **14**, 8715.
- 24 J. H. Zou, S. I. Khondaker, Q. Huo and L. Zhai, *Adv. Funct. Mater.*, 2009, **19**, 479.
- 25 J. Szejtli, *Chem. Rev.*, 1998, **98**, 1743–1753; K. A. Connors, *Chem. Rev.*, 1997, **97**, 1325.
- 26 C. Park, H. Youn, H. Kim, T. Noh, Y. H. Kook, E. T. Oh, H. J. Park and C. Kim, *J. Mater. Chem.*, 2009, **19**, 2310.
- 27 H. Choi, S. O. Kang, J. Ko, G. Gao, H. S. Kang, M.-S. Kang, M. K. Nazeeruddin and M. Grätzel, *Angew. Chem., Int. Ed.*, 2009, **48**, 5938.
- 28 Y. Tang, L. Zhou, J. Li, Q. Luo, X. Huang, P. Wu, Y. Wang, J. Xu, J. Shen and J. Liu, *Angew. Chem., Int. Ed.*, 2010, **49**, 3920.
- 29 J. Shi, Y. Chen, Q. Wang and Y. Liu, *Adv. Mater.*, 2010, **22**, 2575.
- 30 C. Yang, X. Ni and J. Li, *J. Mater. Chem.*, 2009, **19**, 3755.
- 31 A. D. Strickland and C. A. Batt, *Anal. Chem.*, 2009, **81**, 2895.
- 32 R. Freeman, T. Finder, L. Bahshi and I. Willn, *Nano Lett.*, 2009, **9**, 2073.
- 33 Y.-L. Zhao, L. Hu, J. F. Stoddart and G. Grüner, *Adv. Mater.*, 2008, **20**, 1910.
- 34 R. B. C. Jagt, R. F. Gó mez-Biagi and M. Nitz, *Angew. Chem., Int. Ed.*, 2009, **48**, 1995.
- 35 H. Kitagishi, S. Negi, A. Kiriyama, A. Honbo, Y. Sugiura, A. T. Kawaguchi and K. Kano, *Angew. Chem., Int. Ed.*, 2010, **49**, 1312.
- 36 J. Wang, L. T. Kong, Z. Guo, J. Y. Xu and J. H. Liu, *J. Mater. Chem.*, 2010, **20**, 5271.
- 37 A. K. Flatt, B. Chen and J. M. Tour, *J. Am. Chem. Soc.*, 2005, **127**, 8918.
- 38 C. A. Dyke and J. M. Tour, *J. Am. Chem. Soc.*, 2003, **125**, 1156.
- 39 Y. Liu, Z. Yao and A. Adronov, *Macromolecules*, 2005, **38**, 1172.
- 40 Z. Guo, F. Du, D. M. Ren, Y. S. Chen, J. Y. Zheng, Z. B. Liu and J. G. Tian, *J. Mater. Chem.*, 2006, **16**, 3021.
- 41 M. Liu, Y. Yang, T. Zhu and Z. Liu, *Carbon*, 2005, **43**, 1470.
- 42 M. S. Strano, C. A. Dyke, M. L. Usrey, P. W. Barone, M. J. Allen, H. Shan, C. Kittrell, R. H. Hauge, J. M. Tour and R. E. Smalley, *Science*, 2003, **301**, 1519.
- 43 M. C. LeMieux, M. Roberts, S. Barman, Y. W. Jin, J. M. Kim and Z. Bao, *Science*, 2008, **321**, 101.
- 44 T. Hertel, R. E. Walkup and P. Avouris, *Phys. Rev. B: Condens. Matter*, 1998, **58**, 13870.
- 45 D. Qian, E. C. Dickey, R. Andrews and T. Rantell, *Appl. Phys. Lett.*, 2000, **76**, 2868.